

Updates to the Absolute Radiometric Accuracy of the AIRS on Aqua

Thomas S. Pagano*^a, Hartmut H. Aumann^a, Steve Broberg^a, Evan Manning^a, Kenneth Overoye^b, Margaret H. Weiler^b

^aJet Propulsion Laboratory, California Institute of Technology, CA 91109;

^bBAE Systems, Nashua New Hampshire, 03064

ABSTRACT

The Atmospheric Infrared Sounder (AIRS) on the EOS Aqua Spacecraft was launched on May 4, 2002. The AIRS was designed to measure small changes in the global hydro-thermodynamic cycle and has demonstrated exceptional radiometric and spectral stability and accuracy in-orbit. This accuracy is achieved by transferring the calibration from a Large Area Blackbody (LABB) to the On-Board Calibrator (OBC) blackbody during preflight testing. The LABB theoretical emissivity is in excess of 0.9999 and temperature uncertainty is less than 50 mK. The LABB emitted radiance is NIST traceable through thermistors located on the internal surfaces. The AIRS also provides a full aperture space view every scan for offset calibration. AIRS nonlinearity and polarization calibration coefficients were based on pre-flight testing and have been amongst the highest uncertainty sources in the calibration. A recent method using on-board space view data has reduced the uncertainty of the polarization coefficients and use of separate A side and B side data from pre-flight testing has reduced the uncertainty of the nonlinearity estimates. An update to the system radiometric uncertainty is made based on the new data and is presented in this paper.

Keywords: AIRS, hyperspectral infrared, absolute, radiometric, calibration

1. THE ATMOSPHERIC INFRARED SOUNDER

The Atmospheric Infrared Sounder (AIRS) is a hyperspectral infrared instrument on the EOS Aqua Spacecraft, launched on May 4, 2002. AIRS has 2378 infrared channels ranging from 3.7 μm to 15.4 μm and a 13.5 km footprint. The AIRS is a “facility” instrument developed by NASA as an experimental demonstration of advanced technology for remote sensing and the benefits of high resolution infrared spectra to science investigations¹. AIRS, in conjunction with the Advanced Microwave Sounding Unit (AMSU), produces temperature profiles with 1K/km accuracy on a global scale, as well as water vapor profiles and trace gas amounts for CO₂, CO, SO₂, O₃ and CH₄. AIRS data are used for weather forecasting, climate process studies and validating climate models^{2,3}. For more information see <http://airs.jpl.nasa.gov>.

The AIRS instrument, developed by BAE SYSTEMS, incorporates numerous advances in infrared sensing technology to achieve a high level of measurement sensitivity, precision, and accuracy⁴. This includes a temperature-controlled spectrometer (157K) and long-wavelength cutoff HgCdTe infrared detectors cooled by an active-pulse-tube cryogenic cooler. It is this temperature control that is most likely responsible for the observed stability in the instrument. The Focal Plane Assembly (FPA) contains 12 modules with 15 individual PV HgCdTe line arrays of detectors in a 2 x N element arrays where N ranges from 94 to 192 for PV HgCdT, and 2 PC HgCdTe arrays with 1 x 144, 1 x 130 elements. The AIRS acquires 2378 spectral samples at resolutions, $\lambda/\Delta\lambda$, ranging from 1086 to 1570, in three bands: 3.75 μm to 4.61 μm , 6.20 μm to 8.22 μm , and 8.8 μm to 15.4 μm . A schematic of the FPA layout shown in Figure 1. AIRS scans the earth scene up to $\pm 49.5^\circ$ relative to nadir with a spatial resolution of 13.5 km. Each scan provides a full-aperture view of space and an on-board blackbody calibration source. The key to the high accuracy and NIST traceability of AIRS is the high quality On-Board Calibrator (OBC) blackbody. The OBC is a specular coated wedge design with an internal angle of 27.25°.

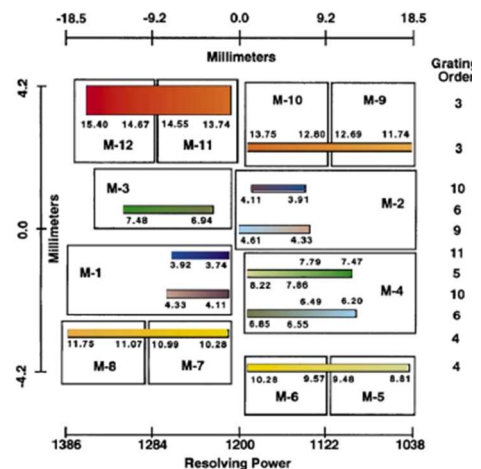


Figure 1. Layout of the AIRS detector modules and their wavelength ranges

*Thomas.S.Pagano@jpl.nasa.gov, (818) 393-3917, airs.jpl.nasa.gov

2. RADIOMETRIC ACCURACY ESTIMATE METHODOLOGY

The radiometric accuracy for AIRS can be determined by combining the error contributions from all the terms in the radiometric transfer equation (conversion of counts to radiance). The results build on prior efforts in the literature including the 2008 SPIE paper estimating the accuracy⁵, and a recent update to the radiometric coefficients and their uncertainties⁶. The new information includes recent measurements in space of the polarization emission from the scan mirror (using space views) and a reanalysis of pre-flight testing data. More information on the pre-flight testing can be found in the literature^{7,8}.

Assumptions: It should be noted that the radiometric analysis discussion in this paper applies to uniform scenes spatially and spectrally consistent with an extended area blackbody. There are no estimates of uncertainty due to the spatial or spectral variability of the scene in this analysis other than that associated with the broad response of the Planck function. If we assume the scene horizontal variability is random, the accuracy estimate applies to very large statistical averages. However we have seen artifacts in the AIRS data due to spatial and spectral response of the instrument that are not corrected in the Level 1B. These artifacts are corrected as best possible at this time in the AIRS Level 1C.

2.1 Radiometric Transfer Equations

The radiometric transfer equations are derived from the design of the AIRS instrument and the measurement approach as discussed in the literature⁶. These radiometric transfer equations form the basis of the Level 1B calibration for AIRS. The scene radiance is computed as a second order polynomial in counts with a term in the denominator due to the mirror polarization.

$$L_{ev} = L_o(\theta) + \frac{c_0 + c_1(dn_{ev} - dn_{sv}) + c_2(dn_{ev} - dn_{sv})^2}{[1 + p_r p_t \cos 2(\theta - \delta)]} \quad (1)$$

$$L_o(\theta) = \frac{L_{sm} p_r p_t [\cos 2(\theta - \delta) - \cos(\theta_{sv,i} - \delta)]}{[1 + p_r p_t \cos 2(\theta - \delta)]} \quad (2)$$

$$c_1' = \frac{[\epsilon_{obc} P_{obc} - L_o(180^\circ)][1 + p_r p_t \cos 2\delta] - c_2(dn_{obc} - dn_{sv})^2 - c_0}{(dn_{obc} - dn_{sv})} \quad (3)$$

where

L_{ev} = Spectral Radiance in the Earth Viewport ($W/m^2-sr-\mu m$)

$L_o(\theta)$ = Polarized Mirror Emission Offset. ($W/m^2-sr-\mu m$)

c_0 = Instrument offset ($W/m^2-sr-\mu m$)

c_1 = Instrument gain ($W/m^2-sr-\mu m$ -counts)

c_2 = Instrument nonlinearity ($W/m^2-sr-\mu m$ -counts²)

dn_{ev} = Digital counts while viewing Earth for each footprint and scan (counts)

dn_{sv} = Digital counts while viewing Space for each scan (counts)

$p_r p_t$ = Product of scan mirror and spectrometer polarization diattenuation (unitless)

θ = Scan Angle measured from nadir (radians)

δ = Phase of spectrometer polarization (radians)

L_{sm} = Spectral Radiance of the Scan Mirror for Unity Emissivity at T_{sm} ($W/m^2-sr-\mu m$)

ϵ_{obc} = Effective Emissivity of the blackbody

P_{obc} = Plank Blackbody function of the OBC blackbody at temperature T_{obc} ($W/m^2-sr-\mu m$)

T_{obc} = Telemetered temperature of the OBC blackbody (K) with correction of +0.3K.

dn_{obc} = Digital number signal from the AIRS while viewing the OBC Blackbody

2.2 Radiometric Uncertainty Analysis

The radiometric uncertainty equation above considers no spatial or spectral errors and should be considered for uniform scenes (spatially) and blackbody distribution of the target (spectrally flat). We discuss the errors associated with spatial and spectral artifacts in section 5. All errors in this analysis are assumed to be 1-sigma since most are computed as standard deviation or RMS differences. The prior analysis in 2008⁵ assumed all errors are 3-sigma, but this analysis revisits the dominant contributors using the old method and the new method and presents all contributors as 2-sigma uncertainties.

The radiometric uncertainty or accuracy can be determined by differentiating the above equation with respect to all the variables. We do this numerically in a computer model by perturbing the nominal values of each variable one at a time with the expected 2-sigma uncertainty and determining the impact on the computed radiance. The root sum square (RSS) is taken on all resulting radiance uncertainties to arrive at a total radiance uncertainty. The process is performed at a

number of different temperatures for each channel of AIRS. Table 1 lists the uncertainty for each term in the calibration equation for the module centered at wavelength of 9.14 μm at a typical scene temperature of 250K. This wave band is highlighted since it occurs at the peak of the polarization of the scan mirror. Also listed in the table is the uncertainty in units of the contributing parameter. We also show the uncertainty in the version 5 (V5) estimate compared to the current version 7k (V7k). The terms adjusted in V7k relative to V5 include the polarization amplitude and phase, the blackbody emissivity and the nonlinearity. We discuss below the individual error contributors and how we derive their uncertainties.

Table 1. Contributors to radiometric uncertainty in AIRS and computed uncertainty for the module centered at 9.14 μm for a scene temperature of 250K. All values are 2-sigma

Parameter	2- σ Uncty	2- σ Uncty	2- σ Uncty (K)	2- σ Uncty (K)
Version	V5	V7k	V5	V7k
Uncertainty in LABB Temperature	0.03 K	0.03 K	0.030	0.030
Uncertainty in LABB Emissivity	0.0001	0.0001	0.0040	0.0040
Uncertainty in Scan Mirror Temperature	1.0 K	1.0 K	0.0067	0.0067
Uncertainty in Polarization Amplitude	0.0013	0.0003	0.076	0.017
Uncertainty in Polarization Phase	0.12 r	0.013 r	0.014	0.0014
Uncertainty in OBC Blackbody Emissivity	0.0017	0.0025	0.065	0.102
Uncertainty in OBC Blackbody Emissivity (EOL)	0.0002	0.0002	0.008	0.008
Uncertainty in OBC Blackbody Temperature	0.05K	0.05K	0.033	0.033
Uncertainty in Nonlinearity	4.09%L@dn _{sat}	1.45%L@dn _{sat}	0.340	0.139
Uncertainty in drift in space view	0.08 dn	0.08 dn	0.004	0.004
Total Uncertainty at Scene Temperature			0.371	0.182

We also present below uncertainties rolled up for all modules and for all channels.

3. DATA

3.1 LABB and SVBB Temperature and Emissivity

The Large Area Blackbody (LABB) is a wedge cavity design used as a warm target during pre-flight testing. The LABB is considerably larger than the OBC blackbody in order to fully illuminate the AIRS aperture from a distance of 11.5" from the scan mirror⁵. The LABB is coated with Aeroglaze Z-302 and the emissivity is estimated to be better than 0.9999. We use 0.0001 for the uncertainty in the analysis. The uncertainty in the LABB temperature has been estimated to be less than 30 mK as determined by the manufacturer (Bomem) in 1996⁹. Errors of up to 200 mK were seen in the zero radiance intercept of the radiometric transfer curve after correction for polarization. This is consistent with model results of the LABB showing highest temperature gradients at cold scene temperatures. For this reason, we do not use the LABB for offset calibration. Offset calibration is performed using in-flight views of space (see section 3.3). LABB testing is only used for calibrating the OBC emissivity, temperature and instrument nonlinearity both of which contribute only at high scene temperatures.

The Space View Blackbody (SVBB) is of similar construction to the LABB with similar emissivity (0.9999) and temperature knowledge (0.5K). Since the SVBB operates at liquid nitrogen temperatures its contribution to the radiometric calibration of emissivity and nonlinearity is negligible.

3.2 Scan Mirror Temperature and Angle

The AIRS scan mirror temperature is monitored using a non-contacting temperature sensor located at the base of the rotating shaft. The uncertainty in the scan mirror temperature is estimated to be less than 0.5K by design; we carry 1K (2-sigma) to allow for design uncertainties in the fabrication of the sensor assembly.

The radiometric uncertainty analysis assumes a nominal scan angle of 0°. The scan mirror angle uncertainty is 1 part in 2¹⁶ due to the encoder and its contribution to the radiometric uncertainty is negligible.

3.3 Polarization Amplitude and Phase

As mentioned above, the AIRS experiences a coupling between the polarization of the scan mirror and the polarization of the spectrometer (dominated by the grating). The coupling modulates the scene radiance slightly (see equation 1), but also leaves a residual error due to the mirror emission that is different when looking in the space view than it is in the Earth view and OBC blackbody view (see equation 2). The correction requires good knowledge of the product of the polarization factor the scan mirror (p_r) and the spectrometer (p_t) and the phase angle between them (δ).

For Version 5, we had individual measurements of the polarization of the scan mirror and completed spectrometer as well as a model that computed the polarization from measurements at the component level. The two models agreed well, except in the longest wavelengths. The approach taken for V5 was to average the measured and component results leaving the uncertainty as the difference between the two. In this uncertainty analysis we use the difference between the two as the uncertainty for V5, whereas in prior uncertainty estimates we used an estimate of 0.002 for all channels⁵. The phase in V5 was assumed to be zero. We know now that not to be the case, so we carry our current estimate for the uncertainty of the phase from V5 as the magnitude of the phase we computed for V7k.

For Version 7k, we compute the polarization amplitude and phase directly from measurements while viewing space⁶. The AIRS obtains 4 views of space at angles of 75°, 82°, 91°, and 101°. We can use these to determine the polarization phase and amplitude by computing the signal difference ($dn-dn_{sv}$) relative to the space view at 91° and solving for the coefficients $p_r p_t$ and δ . Since the AIRS has space view data for every scan for the entire mission, we were able to compute the polarization and phase terms as a function of time. We averaged the space view data into monthly averages to reduce noise and computed a linear fit to the data to give a time dependent polarization and phase term. The uncertainty is computed as 2x the RMS difference between the fit and actual polarization computed at each time interval for each channel.

3.4 OBC Blackbody Emissivity and Temperature

The effective blackbody emissivity is computed by fitting the LABB linearity data preflight and solving for the coefficients c_i . The coefficients are then used in equation 3 to solve for the emissivity. The process is performed on 4 tests obtained preflight: A side electronics, B side electronics for the LABB at nadir and at 40°. The data showed high emissivity but no consistency between the A side, B side, nadir or 40°. The emissivity for V7k was then calculated as the average of all 4 tests. We also perform a 500 channel smooth on the data to remove artifacts that are not expected while viewing a blackbody. The uncertainty is the 2x the standard deviation of the emissivity calculated for the 4 tests relative to the smoothed average. The uncertainty is less than 0.006 for most cases. This is higher than expected with the estimated emissivity of the OBC blackbody of 0.998³, but is most likely due to the uncertainty in the test setup. The estimated degradation at end of life from our prior analysis is also included in the current radiometric uncertainty estimate and is estimated to be 0.0002. Temperature uncertainty of the LABB is estimated to be 0.03K based on knowledge of the temperature sensor calibration⁵.

3.5 Nonlinearity

Nonlinearity is computed by fitting the LABB linearity data preflight to a second order polynomial⁶. The nonlinearity was computed for the four test mentioned in the prior section. In these results it was clearly seen that the A side nonlinearity was consistent between nadir and 40° cases. For this reason, for V7k, we computed the nonlinearity as the average of the A side nadir and 40° data for the A side detectors, and similarly for the B side. 2x the standard deviation of the nadir and 40° cases for each side represents the uncertainty. For V5, the nonlinearity was averaged for A side and B sides and the uncertainty was the difference between the nadir and 40° cases.

3.6 Drift in the Space View

Since the AIRS instrument calibrates once per scan line, we must consider the drift of the offset between calibrations. A measure of this drift was made during the space view noise special test performed pre-launch and in orbit. The drift is calculated as the space view counts at the end of the period (over 600 scans) minus the counts at the start divided by the number of scans in the test period. Typically drift counts are in the range of 0.1-0.5 dn. This drift is converted to a radiometric temperature error using the instrument nominal gain. The same data were used in the prior radiometric uncertainty analysis.

4. RESULTS

Figure 2 shows the results of the radiometric accuracy analysis for all AIRS channels at a scene temperature of 250K. We show version 5 (V5) and version 7k (V7k) results on the same plot to highlight the improvement we now have in the uncertainty. It turns out the coefficients in V5 were pretty good but the uncertainties were higher in most areas. The new in-flight calibration of the polarization using the space view data have improved the polarization coefficients considerably. These new estimates also apply over the entire mission since the polarization is time dependent.

Figure 3 shows module average uncertainties for each of the contributors at 250K scene temperature. Figure 3 (Left) shows the contributors for V5 and Figure 3 (Right) shows the contributors for V7k. For most bands the uncertainties in both versions is dominated by the nonlinearity and OBC emissivity at this temperature (250K). At colder scene temperatures, the polarization dominates the shorter wavelength channels.

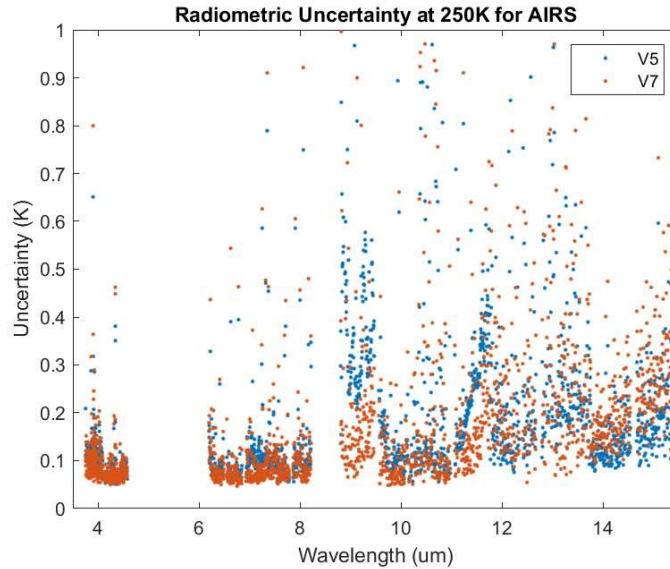


Figure 2. Radiometric Uncertainty for AIRS for a scene temperature of 250K. Reduced uncertainty is seen in most channels.

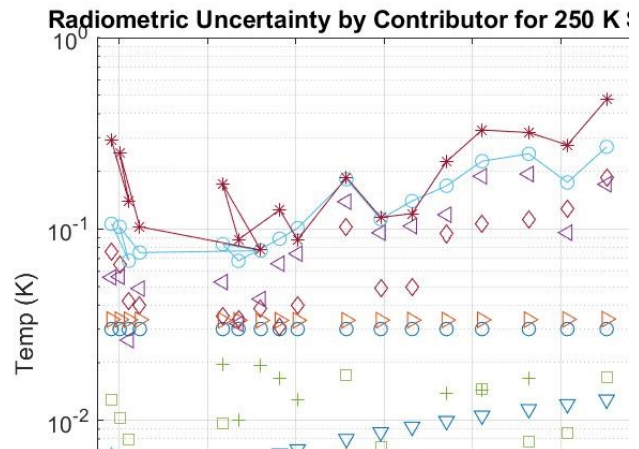
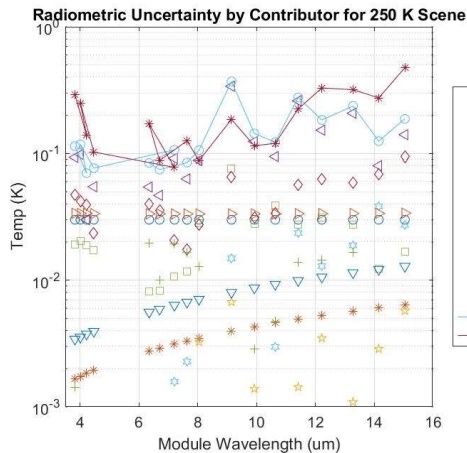


Figure 3. Radiometric uncertainty by contributors for V5 (Left) and V7k (Right) at 250K. The dominant terms are the nonlinearity and OBC emissivity at this temperatures. We see a marked improvement also in the uncertainty of the polarization in V7k particularly at 9 μm . Also shown is the NEDT at 250K for the module average.

Figure 4 shows the total module average uncertainties for V5 (Left) and V7k (Right). This figure highlights many of the improvements in the two versions as well as areas where we have higher uncertainties, mostly because we understand the uncertainties better. First we see the uncertainty at 9.14 μm is better at all scene temperatures except near the OBC temperature of 308K due to better understanding of the polarization and nonlinearity. V7 has higher uncertainty in the OBC emissivity than V5 mainly due to a better estimate of the uncertainty that causes a higher uncertainty for most bands at the OBC temperature. Another band showing marked improvement is the module at 3.8 μm . A better estimate of the polarization improves this band particularly at cold scene temperatures. The band at 12.2 μm shows generally higher

uncertainty than V5, primarily due to the higher uncertainty in the OBC emissivity. For most bands the 2-sigma uncertainty is better than 0.2K, while for the longest wavelengths (>12 μm) the 2-sigma uncertainty is less than 0.3K.

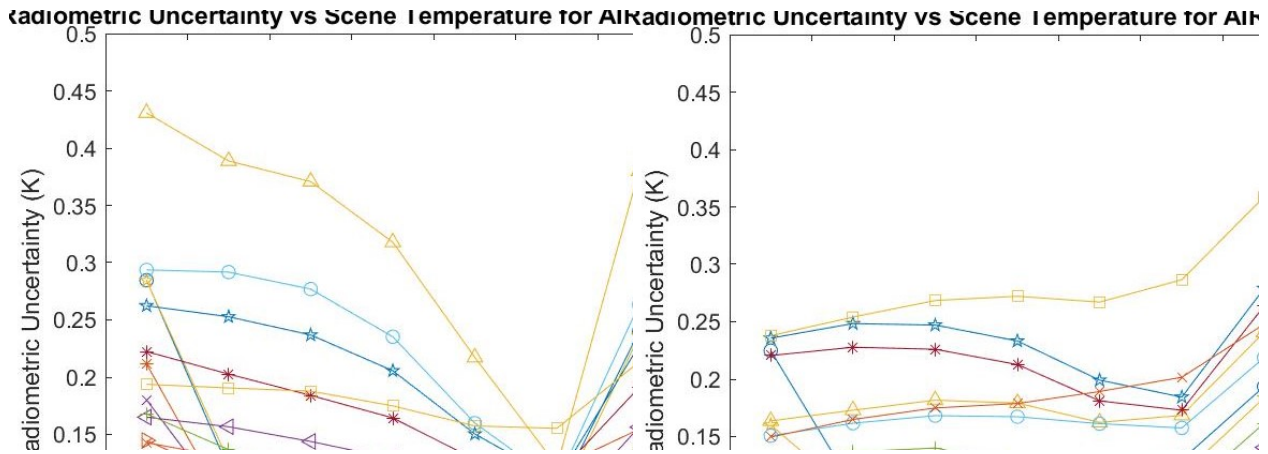


Figure 4. Radiometric uncertainty vs temperature for V5 (Left) and V7k (Right). We see a slight degradation across the board due to the better estimate (but higher) uncertainty of the OBC emissivity in V7k. The improvements due to nonlinearity and polarization are responsible for the improvements seen at cold and warm temperatures for the shortest and longest wave bands.

5. SUMMARY AND CONCLUSIONS

The results show that a significant improvement is achieved in the uncertainty of the calibration for the Version 7k coefficients for most bands. Some bands show slightly lower uncertainty as a result of a better quantification of the uncertainty in the OBC emissivity. The new estimate for V7k assumes 2-sigma uncertainties for all of the contributors.

It should be noted again, that the accuracy estimates described here are for spatially and spectrally uniform scenes and higher errors will result in non-uniform scenes. Effects relating to correlated noise, spatial response inhomogeneity, mirror scatter, spectral knowledge and spectral drift are not included in the analysis.

ACKNOWLEDGEMENTS

The research was carried out at the Jet Propulsion Laboratory, California Institute of Technology, under a contract with the National Aeronautics and Space Administration. © 2018. All rights reserved.

REFERENCES

- [1] T. Pagano, et al., Standard and Research Products from the AIRS and AMSU on the EOS Aqua Spacecraft, Proc. SPIE Vol. 5890, p. 174-183
- [2] J. LeMarshall, J. Jung, J. Derber, R. Treadon, S. Lord, M. Goldberg, W. Wolf, H. Liu, J. Joiner, J. Woollen, R. Todling, R. Gelaro Impact of Atmospheric Infrared Sounder Observations on Weather Forecasts, EOS, Transactions, American Geophysical Union, Vol. 86 No. 11, March 15, 2005
- [3] Pierce D. W., T. P. Barnett, E. J. Fetzer, P. J. Gleckler (2006), Three-dimensional tropospheric water vapor in coupled climate models compared with observations from the AIRS satellite system, Geophys. Res. Lett., 33, L21701, doi:10.1029/2006GL027060.
- [4] Morse, P., J. Bates, C. Miller, Development and test of the Atmospheric Infrared Sounder (AIRS) for the NASA Earth Observing System (EOS), Proc. SPIE, 3759-27, July 1999
- [5] Pagano, T. S., H. Aumann, R. Schindler, D. Elliott, S. Broberg, K. Overoye, M. Weiler, "Absolute Radiometric Calibration Accuracy of the Atmospheric Infrared Sounder", Proc SPIE, 7081-46, San Diego, Ca, August 2008

-
- [6] Pagano, T., Broberg, S., Manning, E., Aumann, H., Strow, L., Weiler, M., "Reducing uncertainty in the AIRS radiometric calibration", Proc. SPIE, 10764-23, August 2018
 - [7] Pagano, T., H. Aumann, D. Hagan, K. Overoye, "Pre-Launch and In-flight Radiometric Calibration of the Atmospheric Infrared Sounder (AIRS)", IEEE TGRS, 41, No. 2, Feb. 2003, p. 265.
 - [8] Pagano, T., H. Aumann, L. Strow, "Pre-launch Performance Characteristics of the Atmospheric Infrared Sounder (AIRS)," SPIE Proc., 4169-41, Sept. 2000
 - [9] AIRS Space View Blackbody and Large Area Blackbody (SVBB & LABB) User's Manual, Bomem, AI-BOM-022/96 Revision A, 14 August 1996